Comparison of strain and ferroelectric properties of La,Nb and Li,Nb co-modified BNKT–ST ceramics

Rizwan Ahmed Malik
University of Engineering and Technology
Adnan Maqbool (adnanmaqbool247@gmail.com)
Changwon National University College of Engineering https://orcid.org/0000-0003-4678-9951
Salman Ali Khan
Changwon National University College of Engineering
Mohsin Saleem
National University of Sciences and Technology School of Chemical and Materials Engineering
Muhammad Shoaib Butt
National University of Sciences and Technology School of Chemical and Materials Engineering
Ibrahim M Alarifi
Majmaah University College of Engineering
Ali Hussain
Institute of Space Technology
Soonil Lee
Changwon National University College of Engineering
Myong-Ho Kim
Changwon National University College of Engineering

Research Article

Keywords: Piezoelectrics; Co-doping; Strain; Ergodicity; Random fields

DOI: https://doi.org/10.21203/rs.3.rs-24755/v1

Abstract

A comparison between the influence of concurrent A and B-site acceptor-donor (Li,Nb) and donor-donor (La,Nb) doping in Pb-free Bi 0.5 (Na 0.84 K 0.16) 0.5 TiO 3 –SrTiO 3 piezoelectrics on structure, ferroelectric and high voltage induced strain were made. In this work, Lithium was chosen as acceptor and Lanthanum was chosen as donor dopant on A-site and Nb 5+ as a B-site donor. Both modifier impurities promoted a phase evolution from the coexistent of two phase structures (rhombohedral-tetragonal) into a more symmetric single pseudocubic structure. Nonetheless, (La,Nb) donor-donor doping induced the phase transition at 1 mol%, while (Li,Nb) acceptor-donor doping at 2 mol%. Interestingly, acceptor-donor (Li,Nb) co-substitution results in the broadening of ergodic relaxor and ferroelectric (ER-FE) mixed phase boundary which is favourable for multidevice applications. This comparative study show that the A-site vacancies play a substantial role to induce the phase transformation from nonergodic-ergodic relaxor (NR-ER) and the improvement in their high voltage induced strain.

Introduction

The emphasis of piezoelectric study during the last decade was given to expansion of lead-free alternative piezoelectric ceramics owing to the environmental issues and laws enacted on the Pb-based (PZT and its solid solutions) piezoceramics [1–3]. Bismuth (Bi^{3+})-based perovskites are the lead-free ceramics which have drawn a huge consideration due to similarity in electronic structure with Pb^{2+}. Bismuth sodium titanate (BNT) ceramic has tempted special interest owing to its environmental friendliness, and good piezoelectric performance. Nonetheless, the problematic poling, low resistivity and high recorded coercive field are the downsides of unmodified BNT [2–4]. Various elemental alterations in pure BNT have been prepared to improve the desired electromechanical properties [5–9]. Among BNT-based binary systems, BNKT is the highly tempting system with relatively better electromechanical performance and morphotrophic phase boundary (MPB) likewise PZT ceramics.

Previous studies on BNKT-based piezoelectric ceramics found that the cation doping induces the hardening and softening effect which can improve the piezoelectric and ferroelectric properties [10–15]. Soft donor doping disrupts the ferroelectric (FE) order by generation of A-site vacancies and increase the dielectric, piezoelectric and electromechanical behavior [16,17]. On the contrary, the hardening effect due to acceptor doping may generate oxygen vacancies and decreasing dielectric constant, loss, and enhancing coercive field and mechanical quality factor [16,17]. Thus, from both academic and industrial viewpoints to probe the impacts of acceptor-donor and donor-donor doping on concurrent A and B-site of BNKT based system have great attraction.

The present work compares the outcomes of concurrent A and B-site acceptor-donor and donor-donor modifications on the phase evolution, ferroelectric, high voltage induced strain and ferroelectric performance of BNKT–ST ceramics.

Materials And Methods

Piezoelectrics $Bi_{0.5}(Na_{0.84}K_{0.16})_{0.5}TiO_3–SrTiO_3$ (x,y = 0.00–0.030) were developed by mixed-oxide reaction. Reagent grade carbonates and oxides (in powders form) of Nb_2O_5, Na_2CO_3, K_2CO_3, TiO_2, La_2O_3, $SrCO_3$, Li_2CO_3 and Bi_2O_3 (~99.9% Sigma Aldrich St. Louis) were utilized. The hygroscopic Na_2CO_3 and K_2CO_3 powders were put in oven at 100°C for 24h. The powders were weighed as per their respective stoichiometric formulae and then put at ball-milling for 24h by utilizing ethanol and zirconia balls. The prepared slurries were heated and calcination was carried out at 850 °C for 2 h. Then, the mixture of powders was put at ball-milling again for 24h and completely dried in oven. Uniaxial pressing was used to produce disc-shaped samples (diameter of 10mm) at 98 MPa. These disc samples were annealed at the temperature of 1160°C with the dwell time of 2h.

Samples were coated by paste of silver and put in furnace at 650°C for the dwell time of 0.5h to form permanent electrodes. Poling process was done in bath of silicon oil by applying dc field of 3-4 kV/mm. X-ray diffraction (XRD, X'pert MPD 3040, Philips, The Netherlands) was utilized in this study to characterize crystal structure analysis. Polarization vs. electric field hysteresis ($P–E$) was analyzed by utilizing ferroelectric tester (Manufactured by Precision LC, Radiant Technologies Inc., Albuquerque, NM). Piezo strain property was recorded by utilizing contact-type sensor for displacement measurement (Millitron; Model 140).

Results And Discussion

XRD Phase analysis were conducted for all sintered specimens of different concentrations, as shown in Figure 1. For unmodified BNKT–ST (x,y = 0.00), the coexistent tetragonal-rhombohedral phases, shown by splitting of peaks at ~40° and ~46°, related to rhombohedral of (111)/(1$\bar{1}$1) peaks and for tetragonal symmetry of (002)/(200) peaks, respectively [18,19]. For both La-Nb and Li-Nb co-doped BNKT–ST piezoceramics, as the doping concentration raised, the splitting of peaks in XRD at around ~40° and ~46° fused into single pseudocubic phase reflection of (111) and (200) peaks, respectively. In case of La-Nb co-doping, the structural phase transition was observed at x,y = 0.010, while Li-Nb co-doped system showed phase transition at x,y = 0.020. This kind of phenomenon was observed previously in BNKT-based piezoceramics modified with Hf [10], Zr [11] and Nb [13].

The comparison of high voltage polarization induced hysteresis ($P–E$) and related composition dependence of remnant polarization (P_r), coercive field (E_c) and maximum polarization (P_m) for La,Nb and Li, Nb co-modified BNKT-ST piezoceramics at ambient temperature (RT) were presented in Fig. 2 and Fig. 3 respectively. For unmodified composition (x,y = 0.00), well-saturated hysteresis with large P_r ~26 μC/cm^2 and E_c ~36 kV/cm values confirm the of E-field dependent irreversible evolution to normal-FE phase from nonergodic relaxor (NR) nano-domain state, good agreement with the relatively abrupt peak of current density (J) displayed in the $J–E$ graphs at $E = E_c$ = 3.1 kV/mm. The x,y = 0.00 composition due to its small local random fields between polar nano-regions (PNRs) is predominantly NR state and

converted rather easily from the randomly oriented frozen nano-domain state into a ordered state of stable long-range FE (NR-FE phase transition) by applying relatively low critical *E*-fields slightly less than E_c and saturated at ~50 kV/cm.

In case of La, Nb co-modification, 1 mol% of La and Nb co-modification partially replace the cations of A and B-site of the host BNKT –ST piezoceramics respectively, due to their comparable ionic sizes. La^{+3} will act as A-site donor [20] and Nb^{+5} [13] as B-site donor, and likely to produce A-site vacancies. The produced vacancies may enhance the local random field and break down the long-range FE order by enhancing local random fields along with four current peaks. Consequently, the reversible transition from FE to ergodic relaxor (ER) state occurs evident by the pinching of corresponding *P–E* loop [21–23]. On the other hand, 1 mol % of Li, Nb co-substitution results in increase of P_r and decrease in E_c with improved ferroelectricity. The role of Nb as a B-site donor may produce the A-site vacancies similar to La, Nb doped ceramic. However Li^+ is expected to enter the A-site (due to its comparable ionic size to Bi, Na, K and Sr) may generate oxygen-vacancies which can be responsible for stabilization of FE order by domain pinning and delay the reversible FE-ER phase transition up to 2 mol% of Li,Nb, as confirmed from relatively sharp corresponding *J–E* curves. The comparison shows that 1mol % Li (acceptor), Nb (donor) doping results in improvement of FE state while 1mol% La (donor), Nb (donor) doping significantly disturb the FE order. Furthermore, the compositions (Li, Nb 0.020 and 0.030), shows almost similar pinching, indicating the broad boundary of strain-generating FE-ER phase transition which is interesting from practical applications point of view. On the contrary, a narrow compositional FE-ER phase boundary was observed for La, Nb 0.010 composition. From these observations, it is suggested that A and B-site concurrent donor doping is more effective to destabilize the long-range FE order rather than the simultaneous A-site and B-site acceptor-donor dopent.

A noticeable difference between the two modifier elements La,Nb and Li,Nb was also observed in their effects on the bipolar strain (*S–E*) loops. Figure 4 displays the strain versus electric field hysteresis curves of La,Nb- and Li,Nb-modified BNKT –ST piezoceramics measured at room temperature. An un-modified BNKT –ST demonstrated a typically butterfly-shaped curve, which has been detected in ferroelectrics [24,25]. The definite value of negative strain (S_{neg}) at both $+E_c$ and $-E_c$ suggests the existence of FE domains, whose orientations switched when the external applied field is reversed. Similar to polarization *P–E* loops, 1mol % La, Nb composition drastically affect the FE long-range order evident by vanishing of S_{neg}. For this composition, the comparable free energy of ER and FE states destabilize FE state under un-biased conditions and the inter-conversion between induced FE domains and nano-domains occur with a comparatively large electric-field-induced strain response and almost zero S_{neg}. On the other hand, 1mol.% Li, Nb concurrent acceptor-donor doping maintained its FE order with the enhancement of S_{neg} and maximum strain (S_{max}) due to the flexible response of domains re-orientation to the external electric field. The S_{neg} is symbolized by the difference between lowest strain points and the zero-field strain of the butterfly loop and the S_{max} corresponds to the strain from zero-field to the maximum electric field (E_{max}) [21]. From strain measurement data, both S_{neg} and S_{max} were calculated and plotted as a function of

dopant contents in Fig. 5. With further donor-donor (La,Nb) co-addition, system transform to a typical ER state. On the contrary, acceptor-donor (Li,Nb) co-substitution results in the delay of onset of ER state and broadened the ER-FE mixed phase boundary which is favourable for industrial applications.

Fig. 6 shows the comparative values of energy storage density (W), energy storage efficiency (η) and low energy loss density (W_{loss}) of both compositions. These are the three important ligands of dielectrics for energy storage applications and determined from *P*– *E* loop by using following equations (see Equations 1 and 2 in the Supplementary Files)

It can be realized from Fig. 6 that a relatively high energy storage density of 0.38 J/cm^3, lower energy loss density (0.14 J/cm^3) along with good efficiency (60%) were observed for La, Nb system at x = 0.020. While for Li, Nb system, the values of energy storage density, loss and efficiency were 0.38 J/cm^3, 0.29 J/cm^3 and 25% respectively. These results suggest that the La, Nb system showed greater energy density properties. The observed energy density values obtained for La, Nb system are comparable to previous results [26–28]. The higher energy density response could be related to the relatively higher P_{max} and small P_r and E_c values.

Conclusion

The present work methodically compared the impacts of co-doping of (La,Nb) and (Li,Nb) on the structural and electrical performance of lead-free BNKT –ST piezoceramics. The acceptor-donor (Li,Nb) and donor-donor (La,Nb) concurrent A and B-site doping exhibited clear differences in ferroelectric and strain and properties. La,Nb co-doping promoted FE to ER transition more strongly with 1mol% La,Nb substitution. On the contrary, 2 mol% Li,Nb co-doping carried a ferroelectric-relaxor crossover, where an abnormal rise in strain property was observed. It is interesting to note that Li,Nb co-modification resulted in compositional stable strain value owing to broadness of FE-ER mix-phase boundary (2 –3mol% Li,Nb doping), which is favorable for multidevice applications. This comparative study show that the A-site vacancies play a substantial role to induce the phase transformation from nonergodic-ergodic relaxor (NR-ER) and the enhancement in their field-induced strain response. Furthermore, relatively good energy density properties were obtained for La,Nb system.

Declaration

Acknowledgement

“This work was supported by the Basic Science Research Program through the National Research Foundation of Korea (NRF), as funded by the National Research Foundation of Korea (NRF) grant funded by the Ministry of Science and ICT (MSIT) (2018R1A2B6005044). This work was also supported by National Research Foundation of Korea (NRF-2018R1D1A1B07041634).”

References

1. Rödel, K.G. Webber, R. Dittmer, W. Jo, M. Kimur, D. Damjanovic, J. Eur. Ceram. Soc. **35**, 1659 (2015)
2. Ullah, R.A. Malik, A. Ullah, D.S. Lee, S.J. Jeong, J.S. Lee, I.W. Kim, C.W. Ahn, J. Eropean Ceram. Soc. **34**, 29 (2014)
3. Zaman, Y. Iqbal, A. Hussain, M.H. Kim, R.A. Malik, J. Mater. Sci. **49**, 3205 (2014)
4. Ullah, C.W. Ahn, R.A. Malik, J.S. Lee, I.W. Kim, J. Electroceram. **33**, 187 (2014)
5. Takenaka, T. Okuda, K. Takegahara, Ferroelectrics. **196**, 175 (1997)
6. Hiruma, Y. Imai, Y. Watanabe, H. Nagata, T. Takenaka, Appl. Phys. Lett. **92**, 262904 (2008)
7. T. Zhang, A.B. Kounga, E. Aulbach, Appl. Phys. Lett. **91**, 112906 (2007)
8. Acosta, J. Zang, W. Jo, J. Rodel, J. Eur. Ceram. **32**, 4327 (2012)
9. Sasaki, T. Chiba, Y. Mamiya, E. Otsuki, Jpn. J. Appl. Phys. **38**, 5564 (1999)
10. Hussain, C.W. Ahn, A. Ullah, J.S. Lee, I.W. Kim, Jpn. J. Appl. Phys. **49**, 041504 (2010)
11. Hussain, C.W. Ahn, J.S. Lee, A. Ullah, I.W. Kim, Sens. Actuator A **158**, 84 (2010)
12. S. Han, C.W. Ahn, I.W. Kim, A. Hussain, J.S. Lee, Mater. Lett. **70**, 98 (2012)
13. N. Pham, A. Hussain, C.W. Ahn, I.W. Kim, S.J. Jeong, J.S. Lee, Mater. Lett. **64**, 2219 (2010)
14. Yuan, S. Zhang, X. Zhou, J. Mater. Sci: Mater. Electron. **20**, 1090 (2009)
15. H. Dinh, M.R. Bafandeh, J.K. Kang, C.H. Hong, W. Jo, J.S. Lee, Ceram. Inter. **41**, S458 (2015)
16. A. Malik, A. Hussain, A. Maqbool, A. Zaman, C.W. Ahn, J.U. Rahman, T.K. Song, W.J. Kim, M.H. Kim, J. Am. Ceram. Soc. **2015**, 1–7, DOI: 10.1111/jace.13722
17. Jo, E. Erdem, R.A. Eichel, J. Glaum, T. Granzow, D. Damjanovic, J. Rödel, J. Appl. Phys. **108**, 014110 (2010)
18. A. Malik, A. Hussain, J.U. Rahman, A. Maqbool, T.K. Song, W.J. Kim, S.Y. Ryou, M.H. Kim, Mater. Lett. **143**, 148 (2015)
19. A. Malik, J.K. Kang, A. Hussain, C.W. Ahn, H.S. Han, J.S. Lee, Appl. Phys. Exp. **7**, 061502 (2014)
20. H. Dinh, H.Y. Lee, C.H. Yoon, R.A. Malik, Y.M. Kong, J.S. Lee, V.D.N. Tran, J. Korean. Phys. Soc. **62**, 1004 (2013)
21. Wang, A. Hussain, W. Jo, J. Rodel, J. Am. Ceram. Soc. **95,** 2241 (2012)
22. Hao, B. Shen, J. Zhai, H. Chen, J. Appl. Phys. **115**, 034101 (2014)
23. Zou, H. Fan, L. Chen, W. Yang, J. Alloys Compd. **495**, 280 (2010)
24. B. Lee, D.J. Heo, R.A. Malik, C.H. Yoon, H.S. Han, J.S. Lee, Ceram. Inter. **39**, S705 (2013)
25. Maqbool, A. Hussain, R.A. Malik, J.U. Rahman, A. Zaman, T.K. Song, W.J. Kim, M.H. Kim, Mater. Sci. Eng. B **199**, 105 (2015)
26. Wang, X. Lou, T. Xia, S. Tian, Ceram. Inter. **43**, 9253 (2017).
27. Viola, H. Ning, M. J. Reece, R. Wilson, T. M. Correia, P. Weaver, M. G. Cain, H. Yan, J. Phys. D. Appl. Phys. **45**, 355302 (2012).
28. Luo, X. Wang, E. Tian, H. Song, H. Wang, L. Li, ACS Appl. Mater. Interfaces, **9** (23), 19963 (2017).

Figures

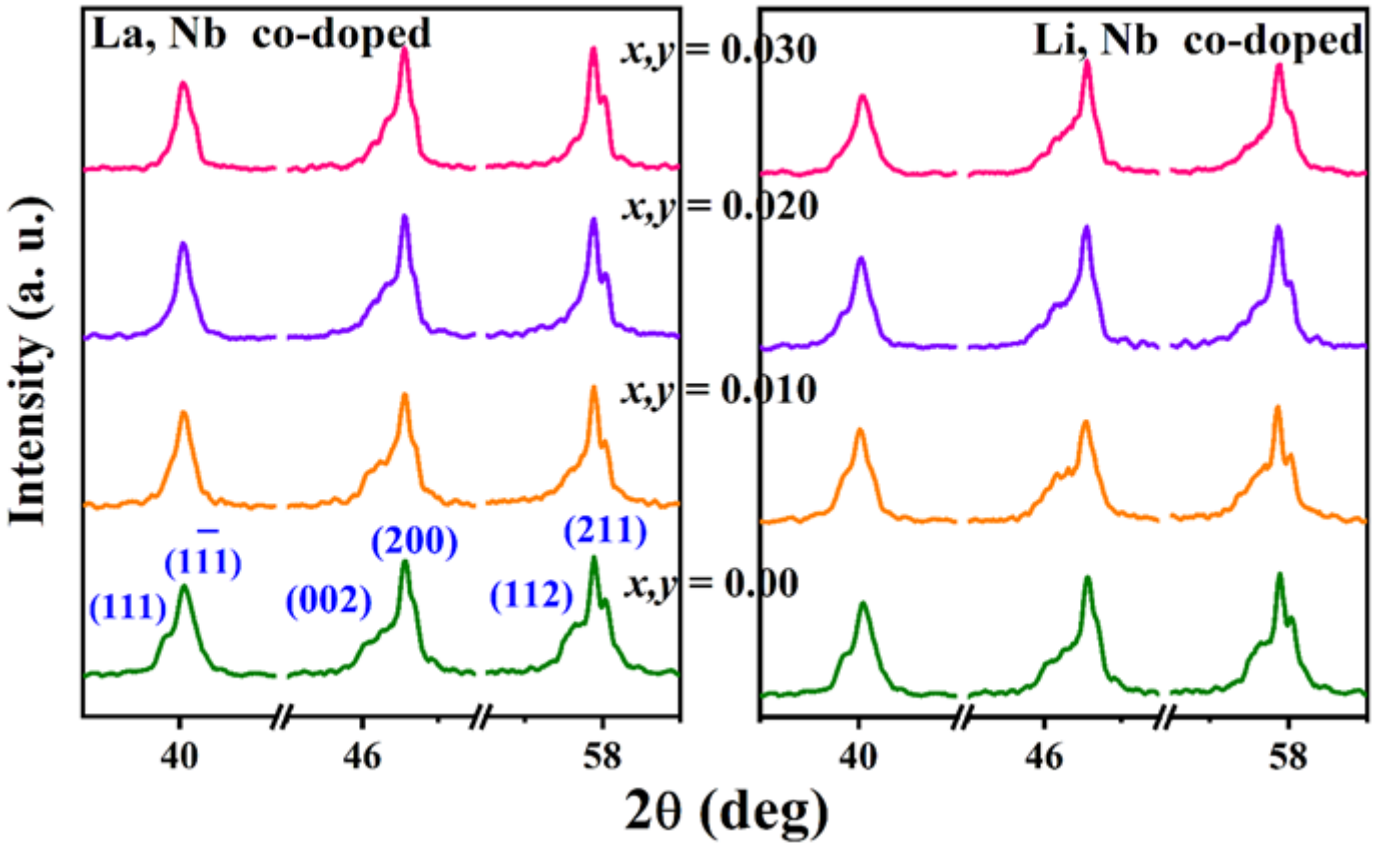

Figure 1

XRD patterns as a function of doping level: (a) La,Nb (b) Li, Nb, for x,y = 0.00–0.030 compositions

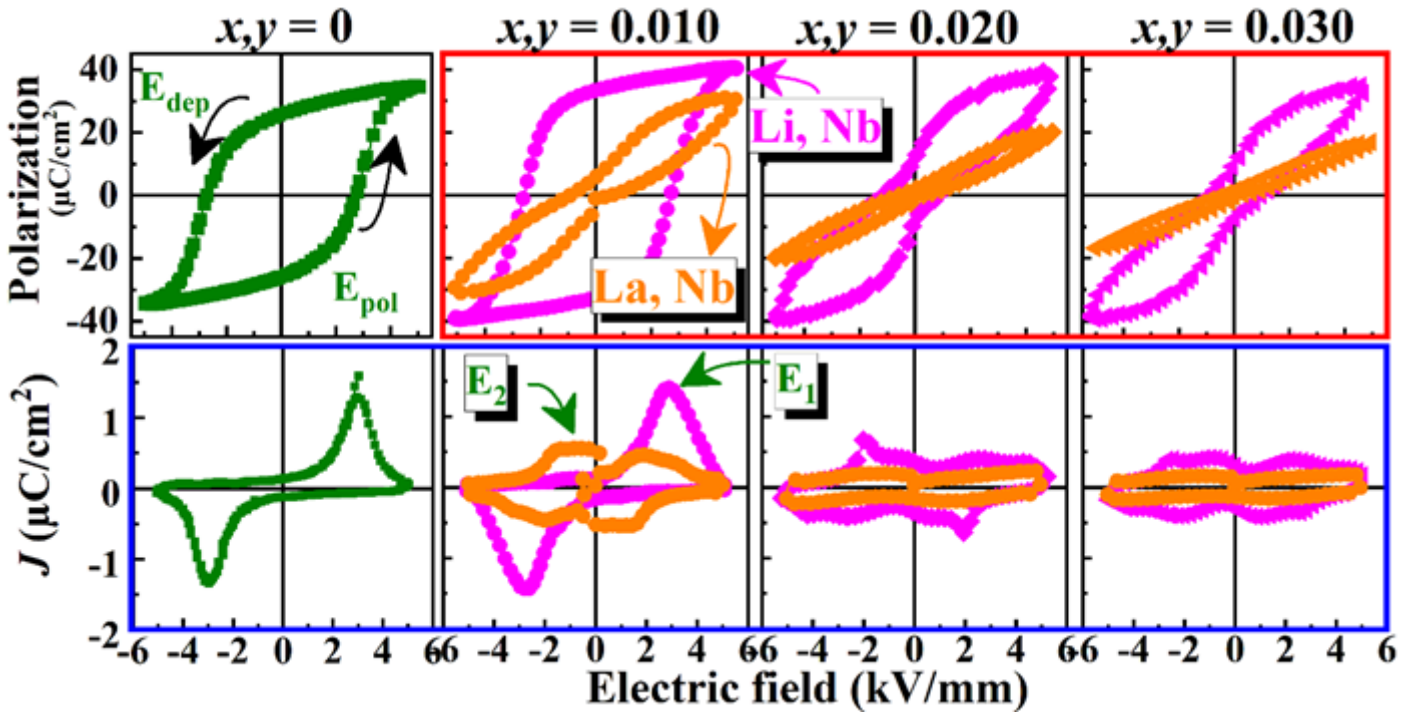

Figure 2

Comparison of La,Nb and Li,Nb co-doping effects on the P–E and J–E hysteresis loop of BNKT–ST ceramics.

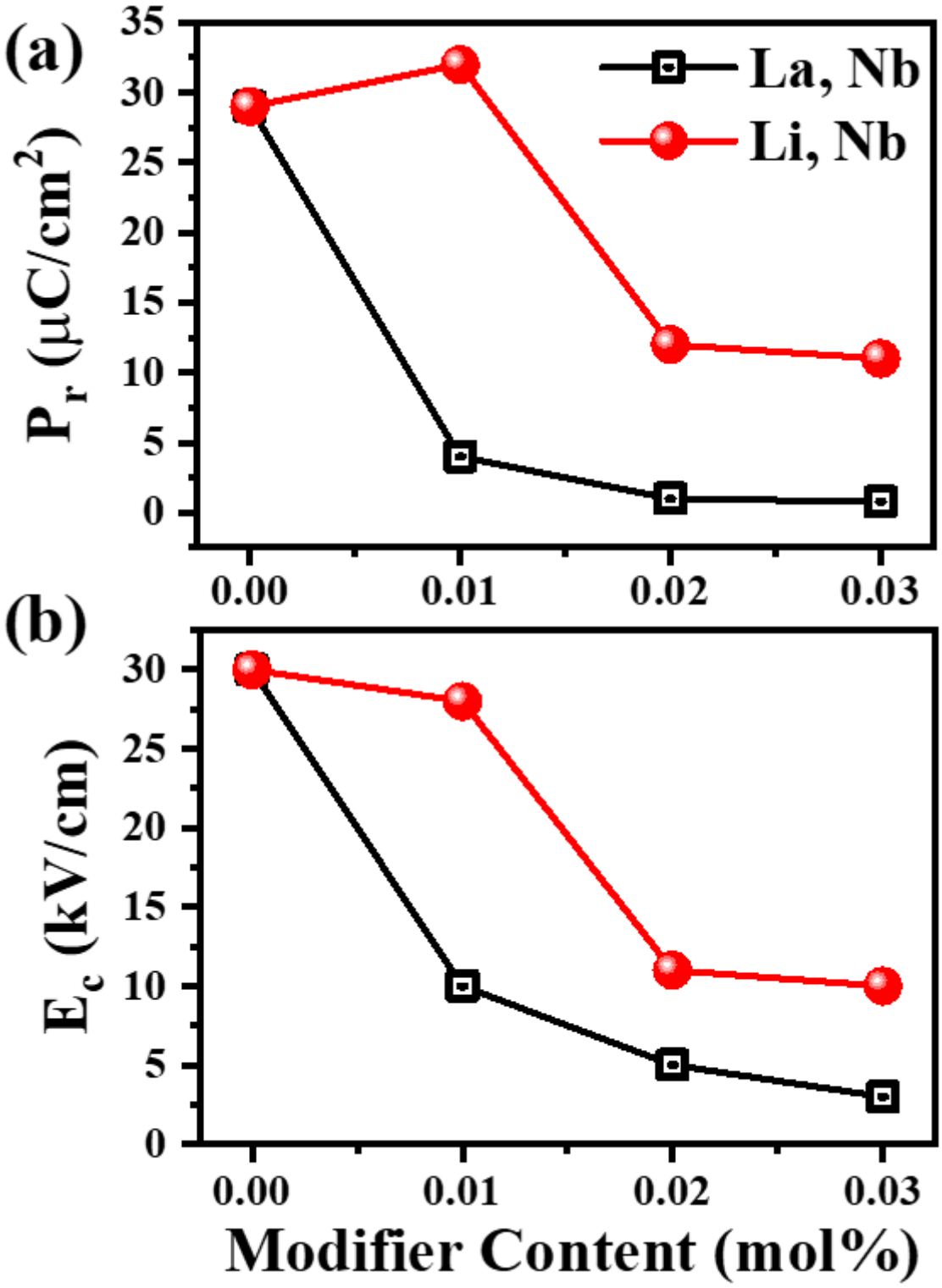

Figure 3

Effect of doping level on (a) the coercive field (Ec), (b) remnant polarization (Pr), of La,Nb and Li,Nb co-doped BNKT–ST ceramics.

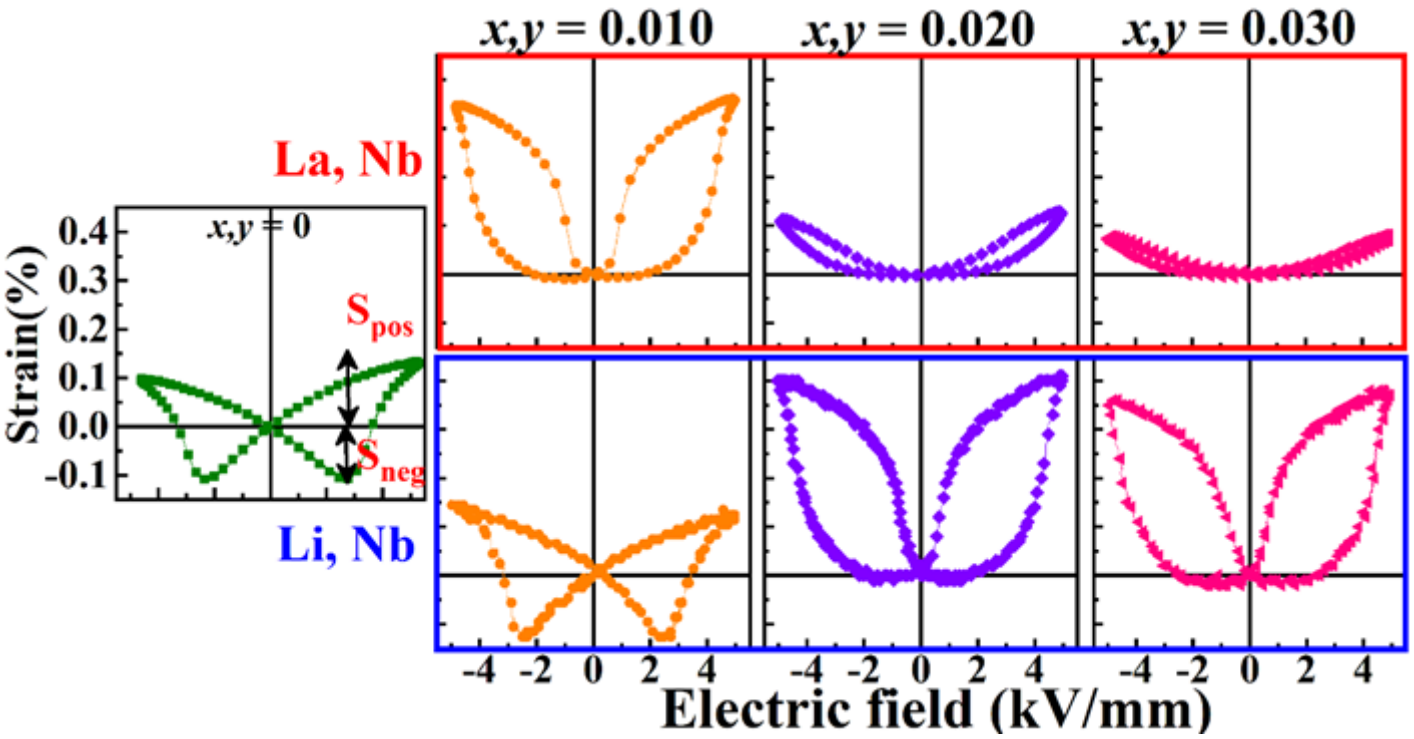

Figure 4

Effect of dopant contents (La,Nb and Li,Nb) on the bipolar S–E hysteresis loops of BNKT–ST ceramics.

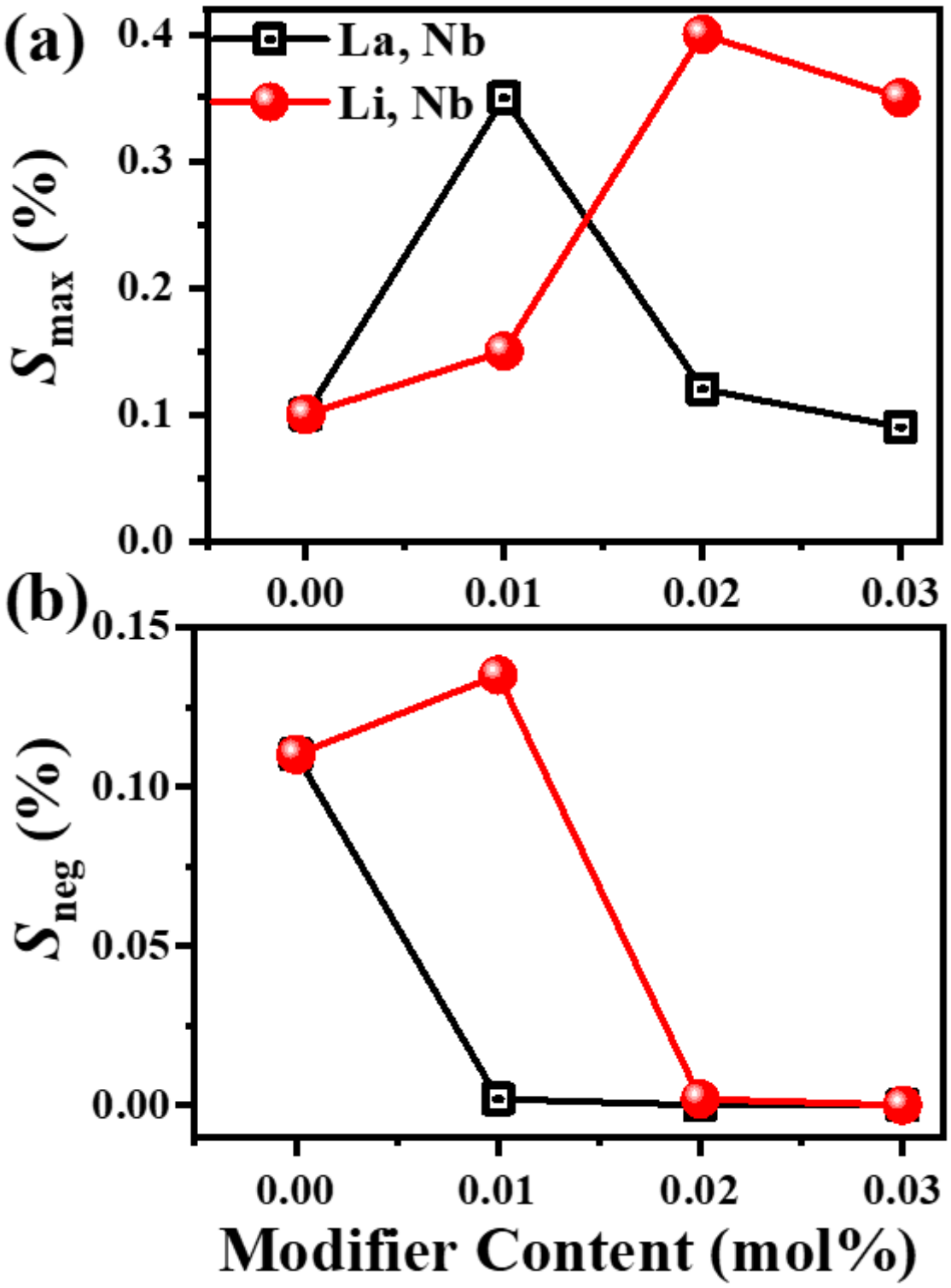

Figure 5

Variation of (a) negative strains (Sneg) and (b) maximum strain (Smax) as a function of La,Nb and Li,Nb co-dopants.

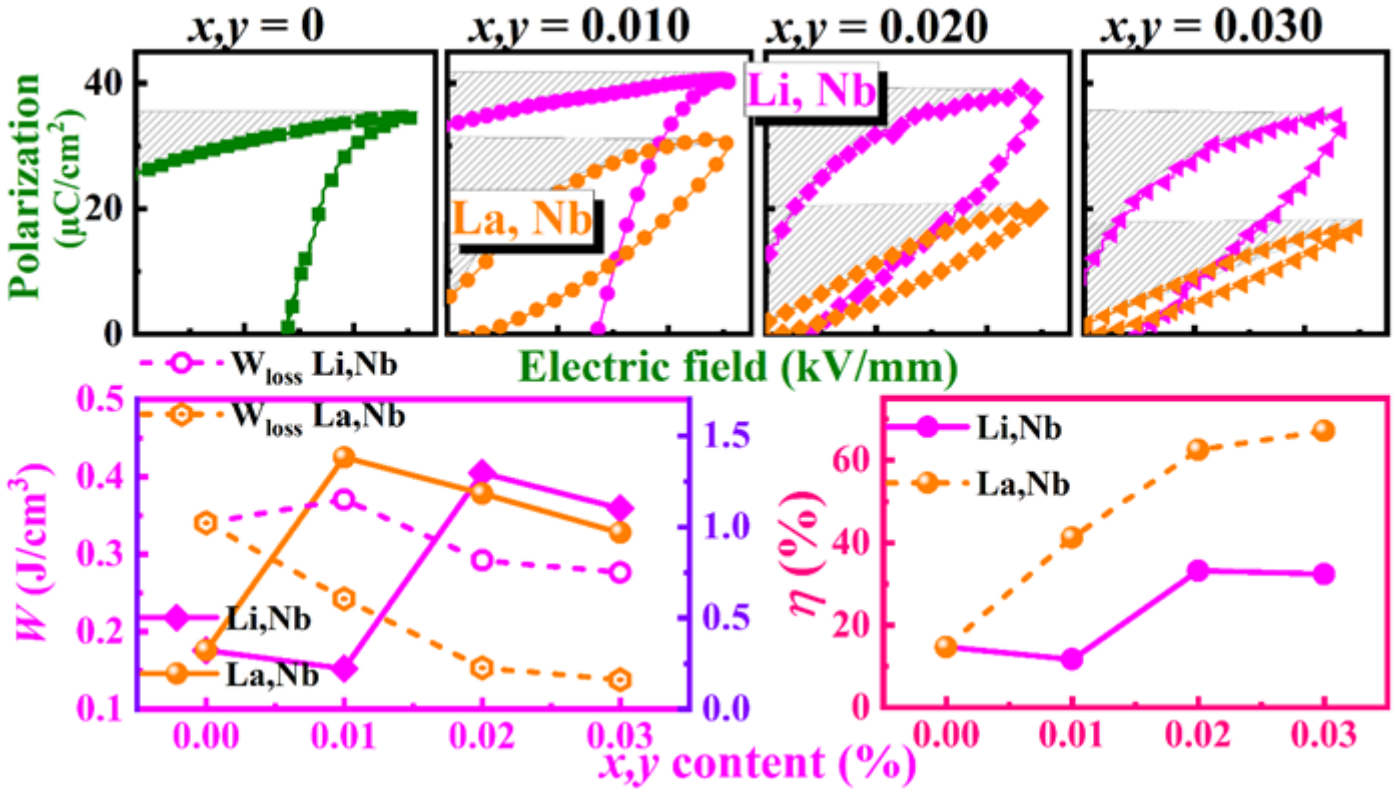

Figure 6

Calculated energy Storage density, loss and efficiency of La,Nb and Li,Nb co-dopants.

Supplementary Files

This is a list of supplementary files associated with this preprint. Click to download.

- Equations.pdf